ScIsoX: A Multidimensional Framework for Measuring Transcriptomic Complexity in Single-Cell Long-Read Sequencing Data

Siyuan Wu[1,2,3] and Ulf Schmitz[1,2,*]

[1]Computational Biomedicine Lab, College of Science and Engineering, James Cook University, Townsville, Queensland, Australia

[2]Centre for Tropical Bioinformatics and Molecular Biology, James Cook University, Cairns, Queensland, Australia

[3]School of Mathematics, Monash University, Melbourne, Victoria, Australia

[*]Corresponding author: Ulf.Schmitz@jcu.edu.au

Tuesday 29th April, 2025

Abstract

Single-cell long-read sequencing enables comprehensive characterisation of full-length transcript isoforms, but lacks robust analytical frameworks for measuring transcriptomic complexity. Here, we introduce `ScIsoX`*, a computational framework that integrates a novel hierarchical data structure, complexity metrics, and visualisation tools for isoform-level investigations.* `ScIsoX` *enables systematic interrogation of global and cell-type-specific isoform expression patterns resulting from splicing, revealing distinct complexity signatures across diverse datasets that were previously inaccessible with short-read approaches.*

Despite revolutionising our understanding of cell type heterogeneity, short-read single-cell RNA sequencing cannot reliably capture full-length transcripts, limiting our ability to resolve complex isoform expression patterns. Alternative splicing dramatically expands the functional repertoire of eukaryotic cells by generating diverse transcript isoforms from a limited number of genes. Recent advances in single-cell long-read sequencing (SCLRS) have enabled comprehensive profiling of full-length transcript isoforms at unprecedented resolution [1]. However, analytical frameworks for measuring and interpreting the multidimensional nature of transcriptomic complexity at single-cell resolution do not exist. This represents a missed opportunity to leverage the additional layers of information provided by SCLRS data, which this study aims to address.

Current approaches for analysing SCLRS data face two major challenges. First, conventional data structures, such as gene-by-cell count matrices, inherently fail to capture the complexity and variability of isoform usage across genes. Attempts to merge gene-level and isoform-level count matrices into

a "cell × gene × isoform" tensor necessitate extensive zero-padding to accommodate gene-specific variability in isoform numbers, resulting in sparse 3D tensors with excessive memory demands. Second, while existing analytical methods excel at isoform discovery and quantification [2, 3], they lack comprehensive metrics that address fundamental questions about the organisational principles governing isoform expression patterns across cells and cell types.

To address these challenges, we introduce `ScIsoX`, a computational framework that implements (i) a novel Single-Cell Hierarchical Tensor (SCHT) data structure, (ii) a comprehensive suite of analytical metrics, and (iii) visualisation tools for measuring transcriptomic complexity across multiple biological scales (Fig.1a and Supplementary Fig.1). At its core, SCHT organises isoform-level count data into gene-specific sub-tensors, where each gene is represented by an individual count matrix containing isoform-by-cell expression values. This partition-based design preserves the intrinsic hierarchy without resorting to extensive zero-padding, yielding a representation that is both biologically meaningful and computationally efficient. When cell type information is integrated, SCHT is extended to include cell types as an additional dimension. Each count matrix contains only the cells belonging to that particular cell type expressing the gene, creating a multi-level hierarchy that elegantly captures gene-isoform-cell relationships.

Building upon this structure, `ScIsoX` conceptualises transcriptomic complexity through seven core metrics, each capturing a distinct dimension of isoform expression patterns (Fig.1a and Supplementary Table 1). The primary dimensions include (I) intra-cellular isoform diversity (i.e., the tendency for a gene to co-express multiple isoforms across the whole cell population), (II) inter-cellular isoform diversity (i.e., the diversity of isoforms expressed by a gene across the whole cell population), (III) intra-cell-type heterogeneity (i.e., cell-to-cell variation in isoform usage), and (IV) inter-cell-type specificity (i.e., measure of cell-type-specific isoform usage). Three additional higher-order metrics measure variability in these patterns to determine, (V) whether cellular heterogeneity is concentrated in specific cell types, (VI) whether cell-type-specific differences occur between particular lineages, and (VII) whether isoform co-expression patterns vary across cell types. To complement these core metrics, we provide additional characterisation metrics that capture specific aspects of isoform usage (Supplementary Table 2).

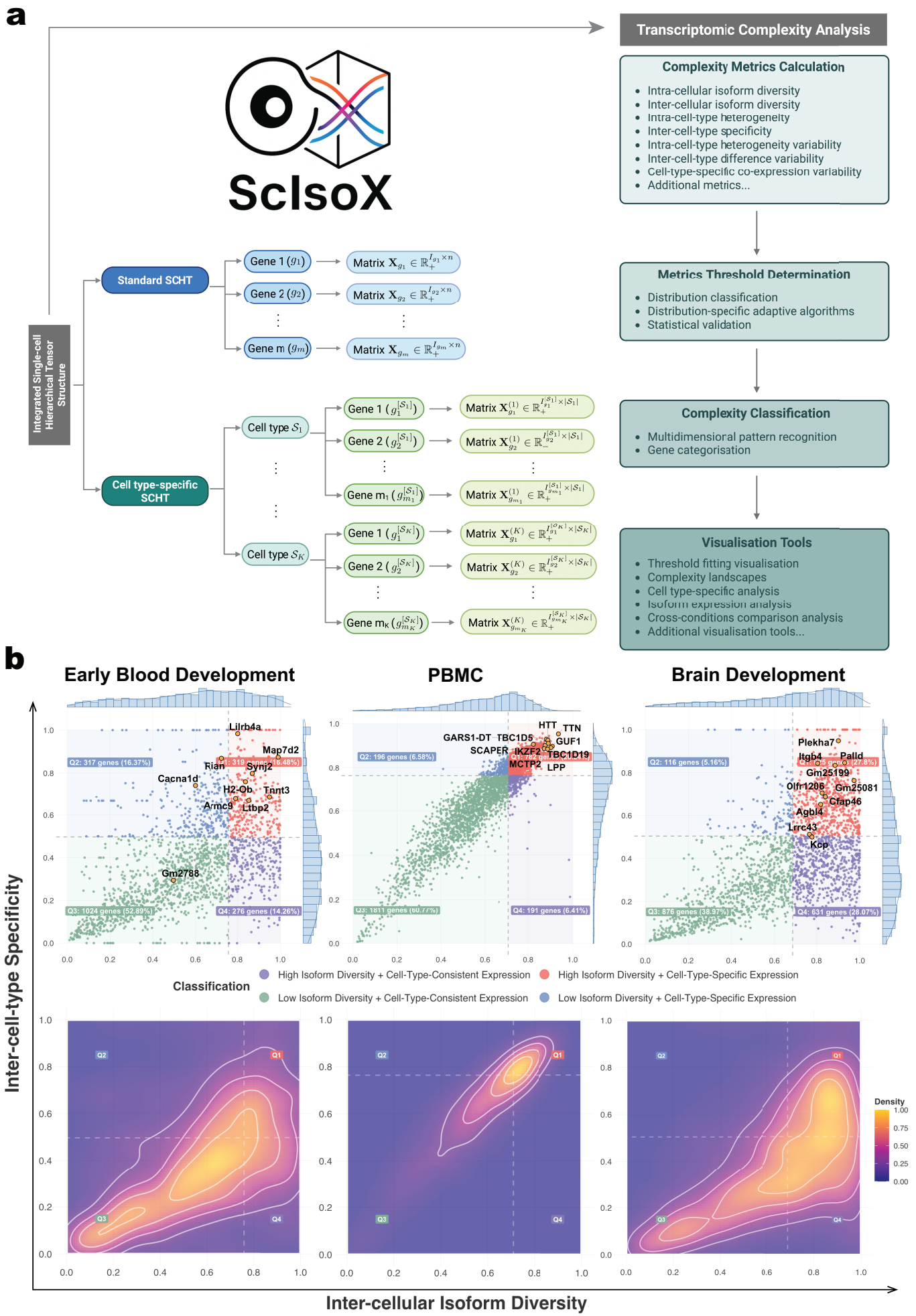
a
ScIsoX
Integrated Single-cell Hierarchical Tensor Structure
Standard SCHT
Gene 1 (g_1)
Gene 2 (g_2)
Gene m (g_m)
Matrix $\mathbf{X}_{g_1} \in \mathbb{R}_+^{I_{g_1} \times n}$
Matrix $\mathbf{X}_{g_2} \in \mathbb{R}_+^{I_{g_2} \times n}$
Matrix $\mathbf{X}_{g_m} \in \mathbb{R}_+^{I_{g_m} \times n}$
Cell type-specific SCHT
Cell type $\mathcal{S}_1$
Gene 1 ($g_1^{[\mathcal{S}_1]}$)
Gene 2 ($g_2^{[\mathcal{S}_1]}$)
Gene m_1 ($g_{m_1}^{[\mathcal{S}_1]}$)
Matrix $\mathbf{X}_{g_1}^{(1)} \in \mathbb{R}_+^{I_{g_1}^{[\mathcal{S}_1]} \times |\mathcal{S}_1|}$
Matrix $\mathbf{X}_{g_2}^{(1)} \in \mathbb{R}_+^{I_{g_2}^{[\mathcal{S}_1]} \times |\mathcal{S}_1|}$
Matrix $\mathbf{X}_{g_{m_1}}^{(1)} \in \mathbb{R}_+^{I_{g_{m_1}}^{[\mathcal{S}_1]} \times |\mathcal{S}_1|}$
Cell type $\mathcal{S}_K$
Gene 1 ($g_1^{[\mathcal{S}_K]}$)
Gene 2 ($g_2^{[\mathcal{S}_K]}$)
Gene m_K ($g_{m_K}^{[\mathcal{S}_K]}$)
Matrix $\mathbf{X}_{g_1}^{(K)} \in \mathbb{R}_+^{I_{g_1}^{[\mathcal{S}_K]} \times |\mathcal{S}_K|}$
Matrix $\mathbf{X}_{g_2}^{(K)} \in \mathbb{R}_+^{I_{g_2}^{[\mathcal{S}_K]} \times |\mathcal{S}_K|}$
Matrix $\mathbf{X}_{g_{m_K}}^{(K)} \in \mathbb{R}_+^{I_{g_{m_K}}^{[\mathcal{S}_K]} \times |\mathcal{S}_K|}$
Transcriptomic Complexity Analysis
Complexity Metrics Calculation
Intra-cellular isoform diversity
Inter-cellular isoform diversity
Intra-cell-type heterogeneity
Inter-cell-type specificity
Intra-cell-type heterogeneity variability
Inter-cell-type difference variability
Cell-type-specific co-expression variability
Additional metrics...
Metrics Threshold Determination
Distribution classification
Distribution-specific adaptive algorithms
Statistical validation
Complexity Classification
Multidimensional pattern recognition
Gene categorisation
Visualisation Tools
Threshold fitting visualisation
Complexity landscapes
Cell type-specific analysis
Isoform expression analysis
Cross-conditions comparison analysis
Additional visualisation tools...
b
Early Blood Development
PBMC
Brain Development
Q2: 317 genes (16.37%)
Q4: 276 genes (14.26%)
Q3: 1024 genes (52.89%)
Lilrb4a
Map7d2
Rian
Synj2
Cacna1d
H2-Ob
Tnnt3
Armc9
Ltbp2
Gm2788
Q2: 196 genes (6.58%)
Q4: 191 genes (6.41%)
Q3: 1811 genes (60.77%)
HTT
TTN
GARS1-DT
TBC1D5
GUF1
SCAPER
IKZF2
TBC1D19
MCTP2
LPP
Q2: 116 genes (5.16%)
Q4: 631 genes (28.07%)
Q3: 876 genes (38.97%)
Plekha7
Itgb4
Palld
Gm25199
Olfr1206
Gm25081
Cfap46
Agbl4
Lrrc43
Kcp
Classification
High Isoform Diversity + Cell-Type-Consistent Expression
High Isoform Diversity + Cell-Type-Specific Expression
Low Isoform Diversity + Cell-Type-Consistent Expression
Low Isoform Diversity + Cell-Type-Specific Expression
Q1
Q2
Q3
Q4
Density
Inter-cell-type Specificity
Inter-cellular Isoform Diversity

Figure 1: **ScIsoX overview and comparison of complexity landscapes across biological systems.** (a) Core of the ScIsoX computational framework showing the interconnected components of data structure and analytical processing. Left: SCHT construction organises isoform expression data into gene-specific sub-tensors; Right: ScIsoX's analytical pipeline progressing from complexity metrics to biological insights. (b) Complexity landscapes in mouse early blood development, human peripheral blood mononuclear cell, and brain datasets, illustrating the relationship between selected complexity dimensions. Upper: The visualised complexity space reveals gene distribution across four quadrants, with annotated genes of interest that demonstrate characteristic complexity signatures; Lower: Density contour maps revealing system-specific clustering patterns, demonstrating how complexity distributions vary across different biological contexts.

We have confirmed ScIsoX's utility by analysing three distinct SCLRS datasets surveying: (1) murine haematopoietic development via Nanopore sequencing [4], (2) murine and human brain development via Nanopore sequencing [5], and (3) human peripheral blood mononuclear cells (PBMCs) via PacBio's Kinnex protocol [6]. These datasets represent fundamentally different biological systems while also employing distinct technical approaches to long-read sequencing. This selection enabled comprehensive evaluation of our framework's performance and broad applicability. All datasets included robust cell type annotations for analysis. Our analysis revealed markedly different transcriptomic complexity patterns in these systems, highlighting the biological insights uniquely accessible through our approach.

The transcriptomic complexity analysis implemented in ScIsoX can, for example, assess four distinct isoform expression patterns: (1) high isoform diversity with high cell type specificity (Q1), (2) low isoform diversity with high cell type specificity (Q2), (3) low isoform diversity with low cell type specificity (Q3), and (4) high isoform diversity with low cell type specificity (Q4) (Fig.1b). These patterns were non-randomly distributed, with murine haematopoietic development exhibiting a bimodal pattern dominated by Q3 (52.89%) with fewer genes showing cell-type-specific expression (Q1+Q2: 32.85%) (Fig.1b). The mouse brain development dataset exhibited a similar bimodal pattern, also demonstrating substantial diversity across quadrants with notable clusters. In contrast, human PBMC dataset exhibited a strikingly different distribution compared to other two development datasets, showing a remarkably strong correlation between inter-cellular isoform diversity and inter-cell-type specificity, with genes predominantly distributed along a diagonal axis from low diversity/low specificity to high diversity/high specificity (Fig.1b). This tight correlation suggests that in specialised immune cells, isoform diversity is closely linked to cell-type-specific functions. Both developmental datasets showed greater range of specificity/diversity relationships than PBMCs, reflecting greater transcriptomic heterogeneity in development compared to specialised immune cells, which require specific isoform switching for state transitions and cellular signals response. Our framework uniquely identifies genes with interesting complexity profiles that may

be overlooked by conventional SCLRS analysis. For instance, the vast majority of genes in all datasets exhibit higher inter-cellular diversity compared to intra-cellular diversity, demonstrating a fundamental principle: genes tend to express cell-type-specific isoforms rather than multiple isoforms in each cell type (Fig.2a). However, a subset of genes with intra-cellular diversity that is higher than their inter-cellular diversity can be identified, suggesting coordinated co-expression of multiple isoforms within individual cells rather than cell-specific isoform selection. These genes may require specific interdependent isoform relationships for proper function, representing a distinct regulatory mechanism for further study. For example, while the role of *Sox17* in endothelial-to-haematopoietic transition is well-established [7, 8], the specific significance of its multiple transcript isoforms remains largely unexplored. Our analysis suggests that *Sox17* may utilise coordinated expression of multiple isoforms to achieve its diverse regulatory functions during haematopoietic development.

Co-expression analysis reveals distinct patterns of coordinated isoform expression. For instance, in murine haematopoietic development, the transcription factor *Irf8*, a key interferon regulatory factor critical for myeloid lineage determination and immune cell differentiation [9], shows multiple clusters of co-expressed isoforms (Fig.2b). `ScIsoX` also enables tracking proportions of expressed isoforms across cell types, further highlighted dynamic changes in isoform usage, e.g., across lineages or developmental stages (Fig.2c). In addition, `ScIsoX` facilitates detailed examination of genes' cell-type-specific complexity profiles. For example, the B-lymphocyte antigen *CD20* (encoded by *MS4A1*) exhibits distinctive isoform expression patterns across human PBMCs, with related myeloid cell types like myelocytes and neutrophils showing markedly different isoform preferences (Fig.2d), suggesting specialised isoform-mediated functions across immune cell lineages. Notably, *MS4A1* falls below the diagonal in diversity analysis (Fig.2a), suggesting its function depends on the orchestrated interplay of multiple isoforms across diverse immune cell types.

Unlike existing approaches that treat isoform diversity as a single dimension, `ScIsoX` provides both a multifaceted view of transcriptomic complexity (Fig.2e and Supplementary Fig.2 - 3) and enables researchers to generate testable hypotheses about the functional significance of alternative splicing, such as across developmental timepoints or anatomical regions. For example, `ScIsoX` reveals distinct patterns of intra-cellular isoform diversity across postnatal developmental stages, with clear gene clusters exhibiting stage-specific isoform expression profiles. The heatmap illustrates how certain gene groups maintain consistently high diversity (dark purple) throughout development, while others show stage-specific diversity patterns (Fig.2f). Additionally, `ScIsoX` reveals distinct patterns of inter-cellular isoform diversity and inter-cell-type specificity that evolve dynamically throughout brain development and differ markedly between brain regions (Supplementary Fig.4 - 5).

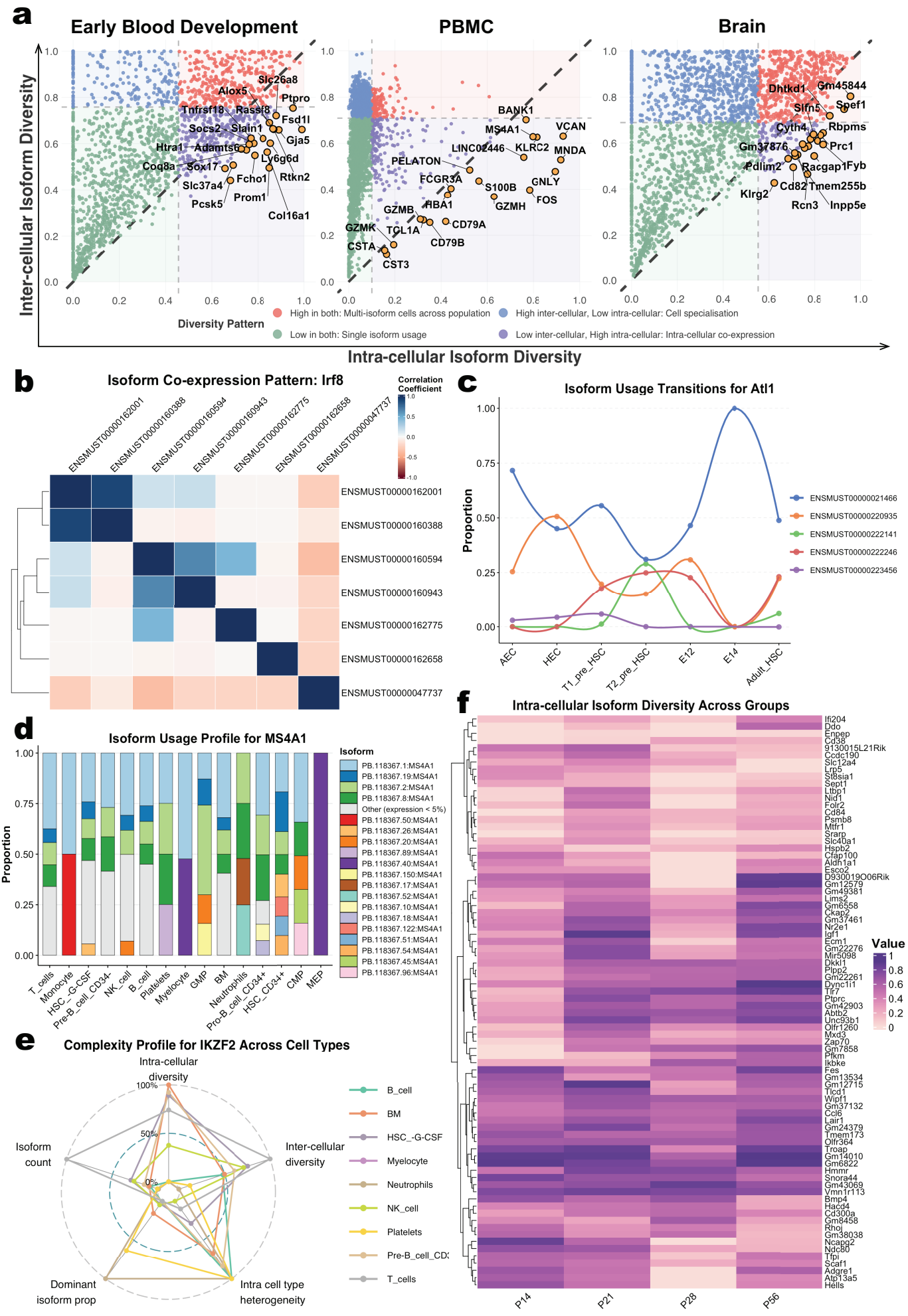
a
Early Blood Development
PBMC
Brain
Inter-cellular Isoform Diversity
Intra-cellular Isoform Diversity
Diversity Pattern
High in both: Multi-isoform cells across population
High inter-cellular, Low intra-cellular: Cell specialisation
Low in both: Single isoform usage
Low inter-cellular, High intra-cellular: Intra-cellular co-expression
b
Isoform Co-expression Pattern: Irf8
Correlation Coefficient
c
Isoform Usage Transitions for Atl1
Proportion
AEC
HEC
T1_pre_HSC
T2_pre_HSC
E12
E14
Adult_HSC
d
Isoform Usage Profile for MS4A1
Isoform
e
Complexity Profile for IKZF2 Across Cell Types
Intra-cellular diversity
Inter-cellular diversity
Intra cell type heterogeneity
Dominant isoform prop
Isoform count
f
Intra-cellular Isoform Diversity Across Groups
Value
P14
P21
P28
P56

Figure 2: **Multidimensional transcriptomic complexity analysis reveals isoform expression patterns.** (a) Intra-cellular versus inter-cellular diversity analysis across three datasets. Highlighted genes falling below the diagonal line (i.e., where intra-cellular diversity exceeds inter-cellular diversity). (b) *Irf8* isoform co-expression correlation analysis, showing both positive and negative expression correlations between different isoforms, suggesting complex regulatory relationships. (c) *Alt1* isoform proportion transitions during mouse haematopoietic development. (d) *MS4A1* isoform usage profiles across different immune cell types in PBMCs. (e) Comparison of *IKZF2* complexity profiles across different immune cell types in PBMCs. (f) Heatmap of intra-cellular isoform diversity across brain postnatal developmental stages (Days 14, 21, 28 and 56).

In summary, `ScIsoX` establishes the first comprehensive framework for measuring and visualising transcriptomic complexity in SCLRS data. Through its hierarchical data structure, `ScIsoX` captures distinct dimensions of transcriptomic complexity at the gene, cell type, and cell population levels, generating insights into transcriptome regulation that were previously inaccessible with short-read technologies. The metrics and visualisations we have implemented provide a foundation for formulating specific questions about the functional roles of alternative splicing in cellular differentiation, cell type specificity, and disease contexts. The adaptable design of `ScIsoX` creates opportunities for future integration with other omics layers and analytical methods, facilitating broad applications in studying alternative splicing regulation, cellular heterogeneity, and cell-type-specific transcriptomic complexity across diverse biological systems. Notably, although our analysis focused on SCLRS data, `ScIsoX` can also analyse isoform count matrices derived from short-read technologies using tools like `Kallisto-bustools` [10]. This compatibility enables researchers to apply our multidimensional complexity framework to existing short-read datasets, though with the caveat that short-read limitations in resolving full-length transcripts may affect some complexity metrics.

Methods

Single-cell hierarchical tensor creation

`ScIsoX` introduces a novel hierarchical data structure that efficiently represents the three-dimensional relationship between genes, isoforms, and cells. Unlike conventional approaches that use either separate gene/transcript matrices, our approach organises isoform-level data into gene-specific sub-tensors. Each gene is represented by an individual matrix containing isoform-by-cell expression values, preserving the intrinsic hierarchy without extensive zero-padding. While we refer to our data structure as a “hierarchical tensor”, we intentionally diverge from the strict mathematical definition, instead adopting a biologically-oriented representation specifically tailored to SCLRS data. This data structure emphasises functional utility and simplicity while facilitating scalable analysis at the isoform level to directly confront the intricacy of transcriptomic complexity.

Quality control and normalisation

Quality control and normalisation were performed in `ScIsoX`. It requires the following inputs: (i) a raw gene count matrix, (ii) a raw isoform count matrix, (iii) a transcript annotation file, and (iv) cell metadata (optional). For the example datasets, quality control was performed at multiple levels: we filtered transcripts that were detected in fewer than $p_{\min}$ proportion of cells (default: 0.02) and with mean expression below ε (default: 1×10^{-6}). At the cell level, we employed a data-adaptive approach to identify and exclude low-quality cells and potential doublets based on the distribution of detected genes. Cells with fewer than $n_{\min}$ genes (default: 200) or more than $n_{\max}$ genes (default: 10,000) were excluded.

Retained count data were normalised using counts per million (CPM) with subsequent logarithmic transformation:

$$x_{gi} = \log_2\left(\frac{c_{gi}}{\sum_{j=1}^{G} c_{gj}} \times 10^6 + 1\right) \tag{1}$$

where c_{gi} represents the raw count for feature g in cell i, and G being the total number of features (genes or transcripts).

Identification of highly variable genes

To prioritise computational resources on genes exhibiting biologically meaningful variation, we implemented a dispersion-based selection of highly variable genes (HVGs). For each gene g, we calculated the variance-to-mean ratio based on their normalised expression counts. We ranked genes by their dispersion values, and the top n_{HVG} genes (default: 3,000) were selected for subsequent analysis. This approach effectively identifies genes with significant biological variability whilst excluding stably expressed housekeeping genes and technical noise. If a greater number of genes is desired for inclusion, n_{HVG} can be increased up to the total number of genes in the dataset.

Mathematical formulation of the SCHT data structure

We developed a hierarchical structure to represent SCLRS data. Let $\mathcal{C} = \{c_1, c_2, \ldots, c_n\}$ be the set of all cells after quality control and filtering, and $\mathcal{G} = \{g_1, g_2, \ldots, g_m\}$ be the set of HVGs. For each HVG $g \in \mathcal{G}$ with I_g isoforms measured across n cells, we define a gene-specific expression matrix:

$$\mathbf{X}_g \in \mathbb{R}_+^{I_g \times n}, \tag{2}$$

where each element $x_{ij} \in \mathbf{X}_g$ represents the normalised expression of isoform i of gene g in cell j. Note that I_g represents the total number of isoforms for gene g, and different genes may have different numbers of isoforms. The standard SCHT data structure is defined as the collection $\mathcal{T} =$

$\{(g, \mathbf{X}_g) \mid g \in \mathcal{G}\}$. Cell-type-specific sub-tensors are created when cell type information is available. We partition the filtered cell set $\mathcal{C}$ into K non-overlapping cell types $\mathcal{S} = \{\mathcal{S}_1, \mathcal{S}_2, \ldots, \mathcal{S}_K\}$. Note that not all genes are expressed in every cell type. For each HVG $g^{[S_k]} \in \mathcal{G}$ that is expressed in cell type $\mathcal{S}_k \in \mathcal{S}$, where $k = 1, 2, \cdots, K$, we denote $I_g^{[\mathcal{S}_k]}$ as the number of isoforms of gene g that are expressed in cell type $\mathcal{S}_k$. We then define a cell-type-specific expression matrix $\mathbf{X}_g^{(k)} \in \mathbb{R}_+^{I_g^{[\mathcal{S}_k]} \times |\mathcal{S}_k|}$ containing columns corresponding to cells of type $\mathcal{S}_k$. The integrated SCHT data structure with cell-type-specific structure is then defined as follows,

$$\mathcal{T}_{\text{integrated}} = \{(g, \mathbf{X}_g, \{\mathbf{X}_g^{(1)}, \mathbf{X}_g^{(2)}, \ldots, \mathbf{X}_g^{(K)}\}) \mid g \in \mathcal{G}\}. \tag{3}$$

This hierarchical representation facilitates comprehensive analysis of transcriptomic complexity.

Multi-dimensional transcriptomic complexity framework

We developed a comprehensive transcriptomic complexity analysis framework that quantifies key aspects of transcriptomic complexity, focusing on a core set of metrics that capture the essential dimensions of isoform expression patterns (Supplementary Table 1).

I: Intra-cellular isoform diversity

To quantify isoform diversity within individual cells, `ScIsoX` computes a weighted Shannon entropy measure for each gene. For cell $c_j \in \mathcal{C}$ expressing gene $g \in \mathcal{G}$, the normalised Shannon entropy is defined as

$$H_j = \frac{-\sum_{i=1}^{I_g} p_{ij} \log_2(p_{ij})}{\log_2(n_j)}, \tag{4}$$

where $p_{ij} = x_{ij} / \sum_{k=1}^{I_g} x_{kj}$ represents the proportion of gene expression attributed to isoform i in cell c_j, and n_j is the number of isoforms detected in that cell. To account for expression magnitude, we compute a weighted mean across cells as intra-celluar isoform diversity,

$$\text{IDI}_{\text{intra}}(g) = \frac{\sum_{j=1}^{n} w_j H_j}{\sum_{j=1}^{n} w_j}, \tag{5}$$

where $w_j = \sum_{i=1}^{I_g} x_{ij}$ is the total expression of gene g in cell c_j. This metric measures the tendency for genes to co-express multiple isoforms across the whole cell population.

II: Inter-cellular isoform diversity

To assess isoform diversity at the cell population level, `ScIsoX` computes the Shannon entropy of the mean isoform expression proportions across all cells, normalised by the maximum possible entropy

as

$$\mathrm{IDI}_{\mathrm{inter}}(g) = \frac{-\sum_{i=1}^{I_g} \bar{p}_i \log_2(\bar{p}_i)}{\log_2(I_g)}, \tag{6}$$

where $\bar{p}_i = \bar{x}_i / \sum_{k=1}^{I_g} \bar{x}_k$, and $\bar{x}_i = \frac{1}{n}\sum_{j=1}^{n} x_{ij}$ is the mean expression of isoform i across all cells. This metric quantifies the overall diversity of isoforms used across the entire cell population.

III: Intra-cell-type heterogeneity

To quantify cell-to-cell variation in isoform usage within a given cell type, `ScIsoX` computes the average Jensen-Shannon distance between cells. For a gene $g \in \mathcal{G}$ expressed in cell type $\mathcal{S}_k \in \mathcal{S}$ with n_k cells, intra-cell-type heterogeneity is defined as

$$\mathrm{Het}_k(g) = \frac{2}{n_k(n_k-1)} \sum_{i=1}^{n_k-1} \sum_{j=i+1}^{n_k} \sqrt{\frac{1}{2}D_{KL}(p_i||m_{ij}) + \frac{1}{2}D_{KL}(p_j||m_{ij})}, \tag{7}$$

where p_i and p_j are the isoform proportion vectors for cells $c_i \in \mathcal{C}$ and $c_j \in \mathcal{C}$ in the cell type $\mathcal{S}_k$, m_{ij} is their average distribution, and D_{KL} is the Kullback-Leibler divergence. The overall intra-cell-type heterogeneity is calculated as the mean across all cell types where the gene is expressed. This metric measures cell-to-cell variation in isoform usage within each cell type. It reveals whether cells of the same type use isoforms consistently.

IV: Inter-cell-type specificity

To assess how distinctly a gene deploys its isoforms across different cell types, `ScIsoX` computes the average Jensen-Shannon distance between cell-type-specific isoform profiles. For a gene $g \in \mathcal{G}$ expressed in S cell types, inter-cell type specificity is defined as

$$\mathrm{Spec}(g) = \frac{2}{S(S-1)} \sum_{i=1}^{S-1} \sum_{j=i+1}^{S} \sqrt{\frac{1}{2}D_{KL}(\bar{p}_i||m_{ij}) + \frac{1}{2}D_{KL}(\bar{p}_j||m_{ij})}, \tag{8}$$

where $\bar{p}_i$ and $\bar{p}_j$ are the vectors of mean isoform proportions for cell types $\mathcal{S}_i \in \mathcal{S}$ and $\mathcal{S}_j \in \mathcal{S}$. Higher values indicate cell-type-specific isoform usage patterns, suggesting specialised functional roles across different cell populations.

V: Intra-cell-type heterogeneity variability

To determine whether cellular heterogeneity is concentrated in specific cell types, `ScIsoX` computes the coefficient of variation (CV) of intra-cell-type heterogeneity values across cell types. For a gene

$g \in \mathcal{G}$ expressed in S cell types, this variability is defined as

$$\mathrm{HetVar}(g) = \frac{\sigma(\{\mathrm{Het}_1(g), \mathrm{Het}_2(g), \ldots, \mathrm{Het}_S(g)\})}{\mu(\{\mathrm{Het}_1(g), \mathrm{Het}_2(g), \ldots, \mathrm{Het}_S(g)\})}, \tag{9}$$

where σ and μ represent the standard deviation and mean, respectively. High values indicate that some cell types have higher internal heterogeneity than others, suggesting targeted subpopulation structure or regulatory plasticity within specific lineages.

VI: Inter-cell-type difference variability

To assess whether isoform usage differences are concentrated between specific cell type pairs, `ScIsoX` computes the CV of pairwise Jensen-Shannon distances. For a gene $g \in \mathcal{G}$ expressed in S cell types, this variability is defined as

$$\mathrm{DiffVar}(g) = \frac{\sigma(\{\mathrm{JS}_{1,2}, \mathrm{JS}_{1,3}, \ldots, \mathrm{JS}_{S-1,S}\})}{\mu(\{\mathrm{JS}_{1,2}, \mathrm{JS}_{1,3}, \ldots, \mathrm{JS}_{S-1,S}\})}, \tag{10}$$

where $\mathrm{JS}_{i,j}$ is the Jensen-Shannon distance between cell types i and j. High values indicate that certain cell type pairs exhibit particularly divergent isoform usage patterns, suggesting lineage-specific splicing regulation or functional specialisation between specific cell populations.

VII: Cell-type-specific co-expression variability

To evaluate whether a gene is subject to different co-expression patterns across cell types, `ScIsoX` computes the CV of mean intra-cellular diversity across cell types. For a gene $g \in \mathcal{G}$ expressed in S cell types, this variability is defined as

$$\mathrm{CoExpVar}(g) = \frac{\sigma(\{\mathrm{IDI}_{\mathrm{intra}_1}(g), \mathrm{IDI}_{\mathrm{intra}_2}(g), \ldots, \mathrm{IDI}_{\mathrm{intra}_S}(g)\})}{\mu(\{\mathrm{IDI}_{\mathrm{intra}_1}(g), \mathrm{IDI}_{\mathrm{intra}_2}(g), \ldots, \mathrm{IDI}_{\mathrm{intra}_S}(g)\})}, \tag{11}$$

where $\mathrm{IDI}_{\mathrm{intra}_k}(g)$ is the mean intra-cellular isoform diversity of gene g in cell type $\mathcal{S}_k$ (i.e., the tendency for genes to co-express multiple isoforms across cell type $\mathcal{S}_k$). High values indicate that a gene exhibits dramatically different co-expression patterns in different cellular contexts, suggesting context-dependent regulation of isoform co-expression.

Additional complexity metrics

`ScIsoX` computes a range of supplementary metrics to further characterise isoform expression pattern. These additional metrics are detailed in (Supplementary Table 2).

Optimal threshold determination for complexity classification

The `ScIsoX` framework implements an advanced multi-stage statistical pipeline to determine optimal classification thresholds for each complexity dimension. This methodology addresses the challenges of analysing heterogeneous distribution patterns observed in transcriptomic complexity metrics.

Distribution-aware preprocessing

For each complexity metric, we first apply distribution-aware preprocessing to identify the underlying distribution characteristics. This preprocessing phase employs multiple statistical approaches:

1. **Distribution classification:** Each metric's distribution is classified into one of several categories: multimodal, zero-inflated, extremely skewed, moderately skewed, or unimodal using a comprehensive multi-method approach. For multimodality detection, we employ three complementary methods, namely Hartigan's dip test for statistical significance, kernel density estimation with adaptive bandwidth selection for peak/valley analysis, and Gaussian mixture modelling with Bayesian Information Criterion for component separation. Skewness is assessed using moment-based calculations with distinct thresholds for moderate and extreme cases.

2. **Zero-inflation detection:** An adaptive histogram-based approach is used to identify zero-inflated distributions. This method calculates a data-dependent near-zero threshold (based on range and interquartile range), determines optimal bin width using the Freedman-Diaconis rule, and analyses the ratio between first and second bins to detect significant zero-inflation. For identified zero-inflated distributions, we further characterise the non-zero component, testing for multimodality and skewness to determine appropriate transformation strategies.

3. **Transformation application:** When necessary, Yeo-Johnson transformations are applied with optimised parameters to normalise extremely skewed distributions while preserving their essential characteristics for threshold determination.

Distribution-specific threshold algorithms

Based on the identified distribution type, specialised algorithms are employed to determine optimal thresholds, with a hierarchical fallback strategy to ensure robust results (Supplementary Fig.6-9):

1. **For multimodal distributions:** our algorithm first attempts to identify inflection points in the density curve, followed by mixture model-based component separation if needed. For distributions with clear valleys between modes, it calculates the optimal separation threshold based on relative depths and positions of these valleys.

2. **For extremely skewed distributions:** our algorithm avoids extreme tails by focusing on the central mass of the distribution, using inflection point and curvature analysis to identify natural separation points.

3. **For zero-inflated distributions:** the non-zero component is extracted and analysed separately, using either gap detection (for significant discontinuities), mixture modelling (for multimodal non-zero components), or adaptive percentiles based on the skewness of the non-zero component.

4. **For moderately skewed and unimodal distributions:** algorithm employs a combination of density curve analysis, distribution moments, and weighted mixtures of normal distributions to identify optimal decision boundaries.

Each method includes reliability assessment, with automatic fallback to simpler techniques when necessary. This adaptive approach ensures robust threshold determination across diverse distribution patterns encountered in complexity metrics.

Statistical validation framework

The reliability of determined thresholds is assessed through a comprehensive validation framework:

1. **Bootstrap stability assessment:** `ScIsoX` performs 100 (adjustable) bootstrap iterations, recalculating the threshold for each resampled dataset. This provides confidence intervals, standard deviations, and coefficients of variation that inform reliability scores, with higher weight given to stable thresholds.

2. **K-fold cross-validation:** For datasets with sufficient samples, `ScIsoX` performs stratified k-fold cross-validation to assess threshold consistency across different subsets of the data. The cross-validation coefficient of variation is integrated into the final reliability assessment.

3. **Distribution-specific reliability adjustment:** Initial reliability scores derived from the primary threshold method are adjusted based on distribution characteristics, with higher penalties for problematic distributions and distributions with limited supporting data.

4. **Sanity checking:** Final thresholds undergo verification against the data distribution's quantiles to ensure they are reasonable, with automated adjustments applied when necessary to prevent threshold placement in extreme distribution tails.

Classification system

Based on the seven core metrics, we developed a multi-dimensional classification system that categorises genes according to their complexity profiles (Supplementary Table 3). For each dimension,

genes are classified into biologically meaningful categories based on the thresholds derived from our distribution-specific threshold algorithms:

1. Intra-cellular isoform diversity is classified as "Strong Isoform Co-expression" or "Weak Isoform Co-expression"

2. Inter-cellular isoform diversity is classified as "High Isoform Diversity" or "Low Isoform Diversity" (see for example in Fig.1b)

3. Intra-cell-type heterogeneity is classified as "High Cellular Heterogeneity" or "Low Cellular Heterogeneity"

4. Inter-cell-type specificity is classified as "Cell-Type-Specific Expression" or "Cell-Type-Consistent Expression" (see for example in Fig.1b)

5. Intra-cell-type heterogeneity variability is classified as "Variable Heterogeneity Across Cell Types" or "Consistent Heterogeneity Across Cell Types"

6. Inter-cell-type difference variability is classified as "High Cell-Type Distinctions" or "Low Cell-Type Distinctions"

7. Cell-type-specific co-expression variability is classified as "Cell-Type-Adaptive Co-expression" or "Cell-Type-Consistent Co-expression"

NA values are preserved throughout this process, as they represent biologically meaningful cases such as single-isoform genes for diversity metrics or genes expressed in only one cell type for inter-cell-type metrics. The integrated classification system enables systematic comparison of transcriptomic complexity patterns across genes and facilitates the identification of genes with interesting or unusual complexity profiles (see example in Supplementary Table 4).

Visualisation and Analysis Features

The `ScIsoX` framework implements a comprehensive suite of visualisation and analysis tools designed to explore and interpret multidimensional transcriptomic complexity patterns. The framework's data structure facilitates efficient analytical workflows that enable researchers to gain biological insights from complex isoform expression patterns.

Core Data Structures and Organisation

The framework organises isoform complexity data into two complementary object structures that support diverse analytical approaches. The `IntegratedSCHT` object encapsulates gene-level isoform expression matrices in a hierarchical structure, with both global and cell-type-specific expression

patterns stored efficiently in a list-based format. The `transcriptomic_complexity` object contains a data frame of complexity metrics (`metrics`), cell-type-specific measurements (`cell_type_metrics`), classification thresholds, and statistical metadata. These data structures, combined with the S3 method system for object manipulation in `R`, enable sophisticated data exploration.

Analytical Tools

1. **Cell-Type-Specific Complexity Analysis** calculates and compares complexity metrics independently for each cell type, enabling the identification of cell types with distinctive isoform regulation patterns.

2. **Complexity Pattern Filtering** identifies genes matching specific combinations of complexity classifications across multiple dimensions using the `find_complexity_pattern()` function. This enables targeted discovery of genes with precise complexity signatures of interest.

3. **Gene Selection Tool** extracts genes with specific complexity characteristics using the `select_genes_of_interest()` function with customisable filtering criteria.

4. **Complexity Metric Comparison** extracts and compare transcriptomic complexity metrics across multiple genes using the `compare_gene_metrics()` function for custom visualisations or statistical analyses.

Visualisation capabilities

1. **Complexity Landscape Visualisations** generate bivariate scatter plots that position genes across two complexity dimensions with integrated marginal distributions. These plots incorporate quadrant statistics and threshold lines to identify genes with exceptional complexity profiles (Fig.1b Top). Interactive highlighting capabilities facilitate the identification of notable genes.

2. **Density Contour Maps** overlay kernel density estimation contours on complexity landscapes to reveal clustering patterns and high-density regions in the complexity space (Fig.1b Bottom). Density contour maps employ adaptive bandwidth algorithms that accommodate varying data densities and highlight regions of biological significance through smooth visualisation of gene concertration hotspots.

3. **Complexity Radar Charts** visualise the complete seven-dimensional complexity signature of individual genes or comparative profiles across multiple genes (Fig.2e and Supplementray Fig.3a). The implementation supports various normalisation methods and custom axis configurations for effective comparison of complexity profiles.

4. **Multi-gene Cell-Type-specific Radar Charts** facilitate the comparison of complexity profiles across multiple genes and cell types in a structured grid layout, enabling the identification of cell-type-specific regulatory patterns (Supplementray Fig.3b). The implementation includes options for global or per-cell type scaling.

5. **Dual Diversity Plots** are scatter plots for intra-cellular and inter-cellular diversity metrics with diagonal reference lines indicating the theoretical equality boundary (Fig.2a). This visualisation specifically highlights genes exhibiting unusual diversity patterns, which may indicate specialised regulatory mechanisms.

6. **Co-expression Correlation Heatmaps** are hierarchically clustered correlation matrices of isoform expression patterns, automatically detecting modules of coordinated or mutually exclusive isoform usage (Fig.2b). The implementation includes options to display correlation values directly.

7. **Isoform Usage Profile Plots** are stacked bar charts that display proportions of expressed isoform usage across cell types, developmental stages, or experimental conditions (Fig.2c). These plots include automatic minor isoform grouping and customisable cell type ordering, facilitating the identification of cell-type-specific isoform preferences.

8. **Isoform Transition Plots** visualise dynamic changes in isoform usage across ordered cell types, time points, or developmental stages (Fig.2d). This approach is particularly effective for revealing isoform switching events during differentiation processes or disease progression.

9. **Ridge Plots** visualise the distribution of complexity metrics through overlapping density curves (Supplementary Fig.2). The implementation supports both global complexity comparisons across metrics and cell-type-specific analyses, offering a compact way to compare multiple distributions simultaneously.

10. **Distribution Threshold Fitting Plots** visualise the distributions of complexity metrics across multiple cell types with optimal threshold determined by the algorithm (Supplementary Fig.6 - 7).

11. **Complexity Metric Heatmaps** provide a comprehensive view of multiple complexity metrics across different groups or conditions (Fig.2f). These heatmaps can be configured to show absolute values or changes between consecutive conditions, with gene selection based on variance, magnitude of change, or custom gene lists.

12. **Group Comparison Density Difference Maps** calculate and visualise the density differences of genes in 2D metric space between different experimental groups or conditions (Supplementary Fig.4 - 5). These visualisations help identify regions where gene distributions shift

across conditions, revealing patterns of coordinated complexity changes in response to experimental manipulations.

All analysis and visualisation functions support comprehensive parameterisation while maintaining computational efficiency for large-scale datasets.

Integration with complementary approaches

The structured organisation of complexity metrics and hierarchical tensor format facilitates integration with complementary single-cell analysis approaches. The quantitative metrics can be correlated with differential expression patterns to identify relationships between expression levels and isoform regulation mechanisms, allowing researchers to relate changes in transcriptomic complexity with expression level alterations across conditions. The transcriptomic complexity signatures can also be correlated with DNA binding motif enrichment patterns to identify potential regulatory elements driving specific complexity profiles. Moreover, the framework's cell type-resolved metrics can be mapped onto trajectory inference results, e.g., to characterise dynamic changes in isoform usage mechanisms during cellular differentiation processes. The classification system enables the incorporation of complexity dimensions into gene regulatory network analyses, potentially revealing how splicing regulators influence network topology and dynamics. Furthermore, these metrics support cross-species comparisons to investigate evolutionary conservation of isoform regulation patterns.

Limitations and considerations

Several limitations should be considered when applying `ScIsoX`. First, some metrics depend on accurate cell type annotation. While the framework is compatible with any popular single-cell clustering and annotation method, the quality of cell type definitions will affect the accuracy of specific metrics, particularly those based on cell type comparisons. In cases where cell type boundaries are ambiguous or annotations uncertain, users should exercise caution when interpreting results or focus on metrics that do not depend on cell type information.

Additionally, users should note that the final number of HVGs in the created SCHT structure may differ from the initial n_{hvg} parameter specified in the `create_scht()` function. This discrepancy occurs because the algorithm removes genes with only a single isoform after processing, ensuring that all genes included in subsequent analyses have multiple expressed isoforms. This filtering step is essential for meaningful isoform complexity analysis but may reduce the final gene count. Improved sequencing quality and depth can significantly mitigate this issue by enabling more comprehensive isoform detection. If researchers wish to maximise the number of genes in downstream analyses, they can increase the n_{hvg} parameter, though this value cannot exceed the total number of genes

present in the dataset.

While the hierarchical data structure offers computational advantages for typical single-cell datasets, extremely large datasets may still require additional optimisation strategies. The framework includes options for batch-wise processing and memory-efficient data handling to address these scenarios.

Cell type annotation

All datasets included robust cell type annotations acquired through different methodologies. For the murine haematopoietic development dataset, cell type annotations were based on experimentally validated labels [4]. For the brain dataset, we utilised preprocessed data and annotations from the study [5]. In that study, computational preprocessing was performed using `Seurat` [11], and annotations were generated through manual marker gene identification. This approach identified major brain cell populations including excitatory and inhibitory neurons, oligodendrocytes, astrocytes, microglia, vascular cells, and progenitor populations. For the PBMC dataset, we also performed preprocessing using `Seurat` [11] and subsequently classified cell types computationally using `SingleR` [12]. The reference dataset contained well-characterised immune cell signatures that enabled identification of T cells, B cells, NK cells, monocytes, and other PBMC subpopulations.

Data Availability

No datasets were generated during the current study.

Code Vailability

ScIsoX is available under the MIT License at https://github.com/ThaddeusWu/ScIsoX

Acknowledgements

U.S. received support from the National Health and Medical Research Council (Investigator Grant #1196405), the Tropical Australian Academic Health Centre (Project Grant SF01124), and the Townsville University Hospital (Grant #THHSSERTA_RPG05_2024, #THHSSERTA_RPG15_2024, and #THHSSERTA_RCG05_2024).

Author Contributions

S.W. and U.S. conceived the topic and structure. S.W. developed the package and drafted the manuscript. U.S. supervised the work and drafted the manuscript. Both authors revised the paper and approved the final version.

Competing Interests

The authors declare no competing interests.

References

[1] Wu, S. & Schmitz, U. Single-cell and long-read sequencing to enhance modelling of splicing and cell-fate determination. *Computational and Structural Biotechnology Journal* **21**, 2373–2380 (2023).

[2] Tian, L. *et al.* Comprehensive characterization of single-cell full-length isoforms in human and mouse with long-read sequencing. *Genome Biology* **22**, 310 (2021).

[3] Kabza, M. *et al.* Accurate long-read transcript discovery and quantification at single-cell, pseudo-bulk and bulk resolution with isosceles. *Nature Communications* **15**, 7316 (2024).

[4] Wang, F. *et al.* Single-cell architecture and functional requirement of alternative splicing during hematopoietic stem cell formation. *Science Advances* **8**, eabg5369.

[5] Joglekar, A. *et al.* Single-cell long-read sequencing-based mapping reveals specialized splicing patterns in developing and adult mouse and human brain. *Nature Neuroscience* **27**, 1051–1063 (2024).

[6] Al'Khafaji, A. M. *et al.* High-throughput rna isoform sequencing using programmed cdna concatenation. *Nature Biotechnology* **42**, 582–586 (2024).

[7] Clarke, R. L. *et al.* The expression of Sox17 identifies and regulates haemogenic endothelium. *Nature Cell Biology* **15**, 502–510 (2013).

[8] Lizama, C. O. *et al.* Repression of arterial genes in hemogenic endothelium is sufficient for haematopoietic fate acquisition. *Nature Communications* **6**, 7739 (2015).

[9] Wang, L. *et al.* The multiple roles of interferon regulatory factor family in health and disease. *Signal Transduction and Targeted Therapy* **9**, 282 (2024).

[10] Melsted, P. *et al.* Modular, efficient and constant-memory single-cell rna-seq preprocessing. *Nature Biotechnology* **39**, 813–818 (2021).

[11] Hao, Y. *et al.* Integrated analysis of multimodal single-cell data. *Cell* **184**, 3573–3587.e29 (2021).

[12] Aran, D. *et al.* Reference-based analysis of lung single-cell sequencing reveals a transitional profibrotic macrophage. *Nature Immunology* **20**, 163–172 (2019).

Supplementary Figures and Tables

Metric	Description	Calculation Method	Biological Interpretation	High Values Indicate	Low Values Indicate
Intra-cellular Isoform Diversity	Measures the tendency for a gene to co-express multiple isoforms across the whole cell population	Weighted average of per-cell normalised Shannon entropy	Reveals whether genes express multiple isoforms simultaneously	Active co-expression of multiple isoforms within individual cells (potential functional cooperation)	Expression of predominantly one isoform per cell (potential mutually exclusive regulation)
Inter-cellular Isoform Diversity	Quantifies the diversity of isoforms expressed by a gene across the whole cell population	Normalised Shannon entropy of average isoform expression	Shows the overall diversity of isoforms expressed in the tissue	Multiple isoforms present across the cell population (diverse functionality)	One or few dominant isoforms across the population (consistent functionality)
Intra-cell-type Heterogeneity	Measures cell-to-cell variation in isoform usage within each cell type	Average Jensen-Shannon distance between cells within a cell type	Reveals whether cells of the same type use isoforms consistently	High cell-to-cell variability in isoform usage (potential sub-populations or states)	Consistent isoform usage pattern within the cell type (consistent functionality)
Inter-cell-type Specificity	Quantifies how differently a gene uses its isoforms across different cell types	Average Jensen-Shannon distance between cell type-specific isoform profiles	Shows whether isoform usage is cell type-specific	Cell types use distinct isoform repertoires (specialised functions)	Similar isoform usage across cell types (conserved functions)
Intra-cell-type Heterogeneity Variability	Measures whether certain cell types show particularly high cellular heterogeneity	Coefficient of variation of heterogeneity values across cell types	Reveals if heterogeneity is concentrated in specific cell types	Some cell types have much higher internal heterogeneity than others (targeted sub-population structure)	Consistent levels of heterogeneity across all cell types (uniform regulation)
Inter-cell-type Difference Variability	Measures whether certain cell type pairs show particularly significant differences	Coefficient of variation of pairwise Jensen-Shannon distances	Shows whether differences are concentrated between specific cell type pairs	Certain cell type pairs have dramatically different isoform usage (lineage-specific divergence)	Relatively uniform differences between all cell type pairs (gradual differentiation)
Cell-type-specific Co-expression Variability	Measures whether a gene exhibits different co-expression patterns in different cell types	Coefficient of variation of mean intra-cellular diversity across cell types	Reveals if co-expression patterns vary by context	Gene exhibits different co-expression patterns in different cell types (context-dependent regulation)	Consistent co-expression mechanism across all cell types (fixed regulatory mechanism)

Supplementary Table 1: **Core Transcriptomic Complexity Metrics**

Metric	Description	Calculation Method	Biological Interpretation
IDI Difference	The difference between inter-cellular and intra-cellular isoform diversity	Inter-cellular isoform diversity – Intra-cellular isoform diversity	Positive values indicate greater diversity across cells than within cells, suggesting cell specialisation; negative values suggest cells co-express many isoforms but in similar patterns
Simpson Index	Alternative diversity measure more sensitive to dominant isoforms	1 - sum(iso_props^2)	Accounts for the probability that two randomly selected transcripts belong to different isoforms; complements Shannon entropy-based metrics
Evenness	Normalised diversity controlling for number of expressed isoforms	inter_cellular_isoform_diversity / log2(n_expressed_isoforms)	Measures how equally expressed the isoforms are; values near 1 indicate equal expression, near 0 indicate dominance by few isoforms
Dominant Isoform Proportion	The proportion of the most abundant isoform	max(iso_props)	Indicates the degree of dominance by a single isoform; high values suggest one functional isoform dominates
Number of Expressed Isoforms	Count of isoforms with detectable expression	sum(iso_means > 0)	Indicates the absolute diversity of isoforms being expressed; reflects the gene's splicing complexity
Percentage of Multi-isoform Cells	Percentage of cells expressing multiple isoforms of a given gene	(Multi-isoform cell count / cells expressing) × 100	Direct measure of co-expression at the single-cell level; high values indicate widespread co-expression
Cells Expressing	Number of cells with detectable expression of a given gene	sum(cell_sums > 0)	Indicates the prevalence of the gene's expression across the cell population
Percentage of Cells Expressing	Percentage of total cells expressing the gene	(cells_expressing / total_cells) × 100	Measures how widespread the gene's expression is; distinguishes ubiquitous from restricted expression patterns

Supplementary Table 2: **Additional Transcriptomic Complexity Metrics**

Dimension	High Classification	Low Classification	Interpretation
Intra-cellular Isoform Diversity	High Isoform Co-expression	Low Isoform Co-expression	Distinguishes genes based on single-cell co-expression patterns
Inter-cellular Isoform Diversity	High Isoform Diversity	Low Isoform Diversity	Distinguishes genes based on population-level isoform diversity
Intra-cell-type Heterogeneity	High Cellular Heterogeneity	Low Cellular Heterogeneity	Distinguishes genes based on cell-to-cell variability within cell types
Inter-cell-type Specificity	Cell Type-Specific Expression	Cell Type-Consistent Expression	Distinguishes genes based on cell type specialisation of isoform usage
Intra-cell-type Heterogeneity Variability	Variable Heterogeneity Across Cell Types	Consistent Heterogeneity Across Cell Types	Distinguishes genes based on targeted vs. uniform heterogeneity
Inter-cell-type Difference Variability	High Cell-Type Distinctions	Low Cell-Type Distinctions	Distinguishes genes based on focused vs. gradual differentiation
Cell-type-specific Co-expression Variability	Cell-Type-Adaptive Co-expression	Cell-Type-Consistent Co-expression	Distinguishes genes based on context-dependent isoform co-expression

Supplementary Table 3: **Metrics Classification System**

Pattern	Biological Significance	Example Genes	Potential Functional Implications
High Intra-cellular Isoform Diversity + High Inter-cellular Isoform Diversity	Rich isoform landscape both within and across cells	Genes involved in complex cellular processes	Multiple functional isoforms with complementary roles; high regulatory complexity
Low Intra-cellular Isoform Diversity + High Inter-cellular Isoform Diversity	Cell specialisation in isoform usage	Cell type marker genes, specialised receptors	Cell type-specific isoform selection; potential for specialised functions
Low Intra-cellular Isoform Diversity + Low Inter-cellular Isoform Diversity	Single dominant isoform usage	Housekeeping genes, core cellular machinery	Conserved function requiring specific isoform; limited need for diversity
High Intra-cellular Isoform Diversity + Low Inter-cellular Isoform Diversity	Consistent co-expression of specific isoform sets	Genes requiring balanced isoform ratios	Functional requirement for multiple isoforms within same cell; potential isoform cooperation
High Cell-type Specificity + Low Difference Variability	Consistent differentiation across all cell types	Lineage-specific transcription factors	Gradual divergence in isoform usage corresponding to cellular differentiation
High Cell-type Specificity + High Difference Variability	Targeted differentiation between specific lineages	Immune recognition molecules, neuronal connectivity factors	Sharp transitions in isoform usage between specific lineages; potential for dramatic functional shifts

Supplementary Table 4: **Example of Complexity Patterns**

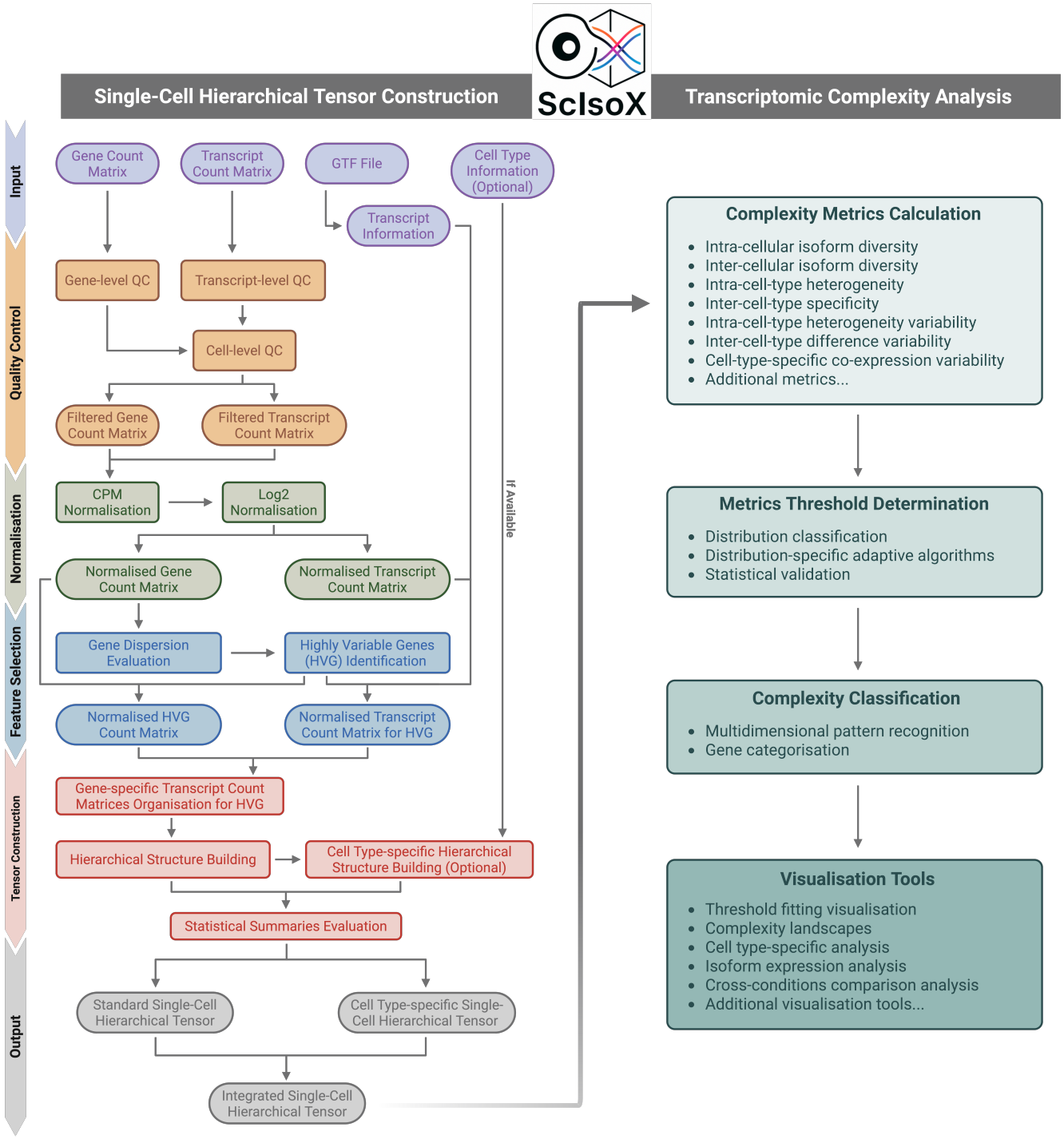

Supplementary Figure 1: **Detailed workflow of the `ScIsoX` analysis framework.** This is the comprehensive overview of the `ScIsoX` analysis pipeline, beginning with input data on the left (gene count matrix, transcript count matrix, GTF file, and cell type information), proceeding through quality control, normalisation, highly variable genes selection, SCHT construction, and culminating in the various components of transcriptomic complexity analysis on the right. The transcriptomic complexity analysis includes complexity metrics calculation (seven core metrics and additional metrics), distribution-based adaptive threshold determination, multidimensional complexity classification, and rich visualisation tools. Each processing step is clearly defined, forming a complete analytical pipeline that supports extraction of biological meaning from SCLRS data.

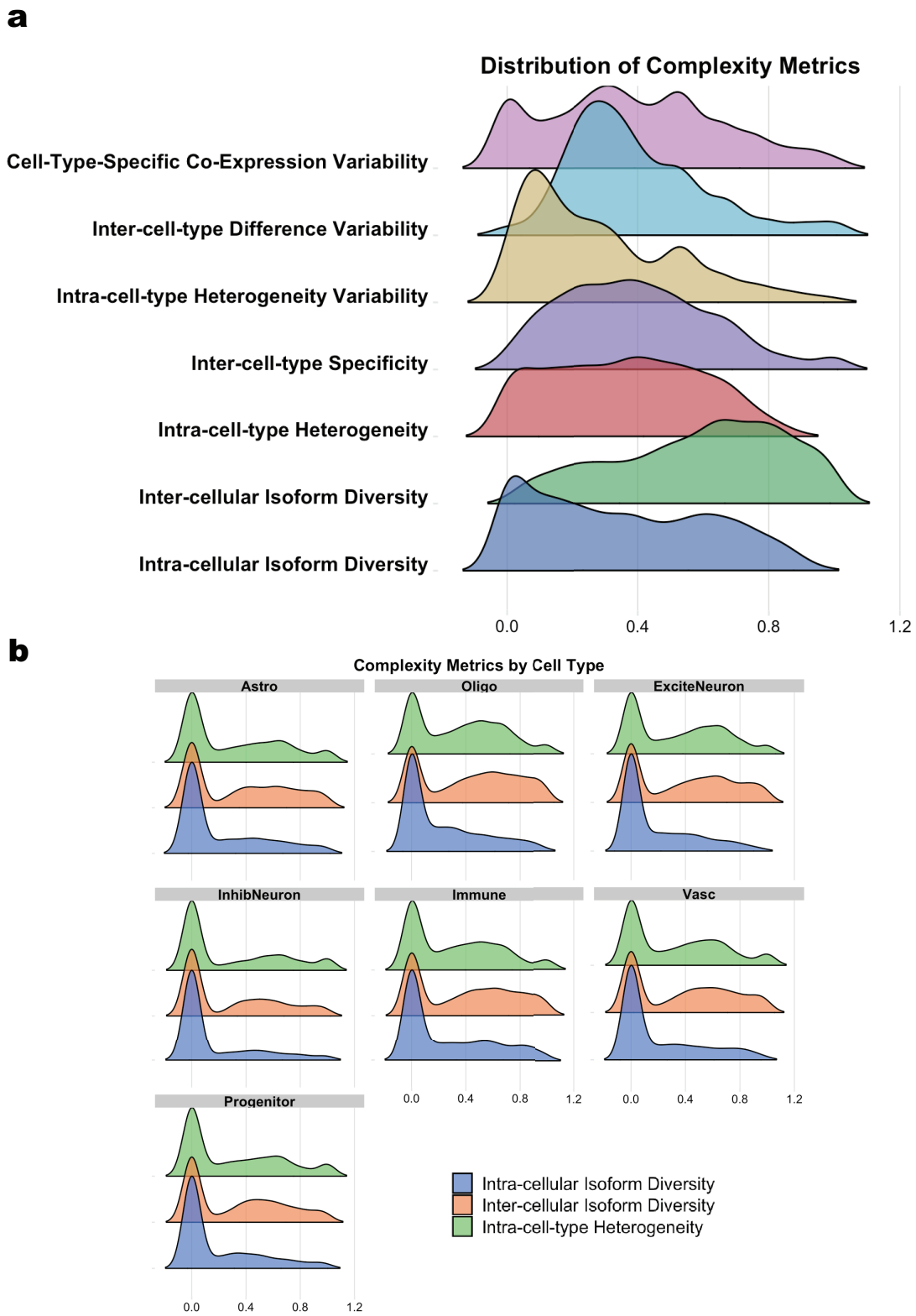

Supplementary Figure 2: **Distribution characteristics of the seven core complexity metrics and cell-type-specific patterns.** (a) Ridge plots showing distributions of the seven core complexity metrics in the brain dataset, displaying characteristic distributions for each dimension. Each metric exhibits a unique distribution profile, reflecting the biological complexity captured by different dimensions. (b) Comparison of density plots for three key complexity metrics across seven cell types in the brain dataset. Immune - immune cells; Astro - astrocytes; Oligo - oligodendrocytes; ExciteNeuron - excitatory neurons; InhibNeuron - inhibitory neurons; Progenitor - progenitor cells; Vasc - vascular cells.

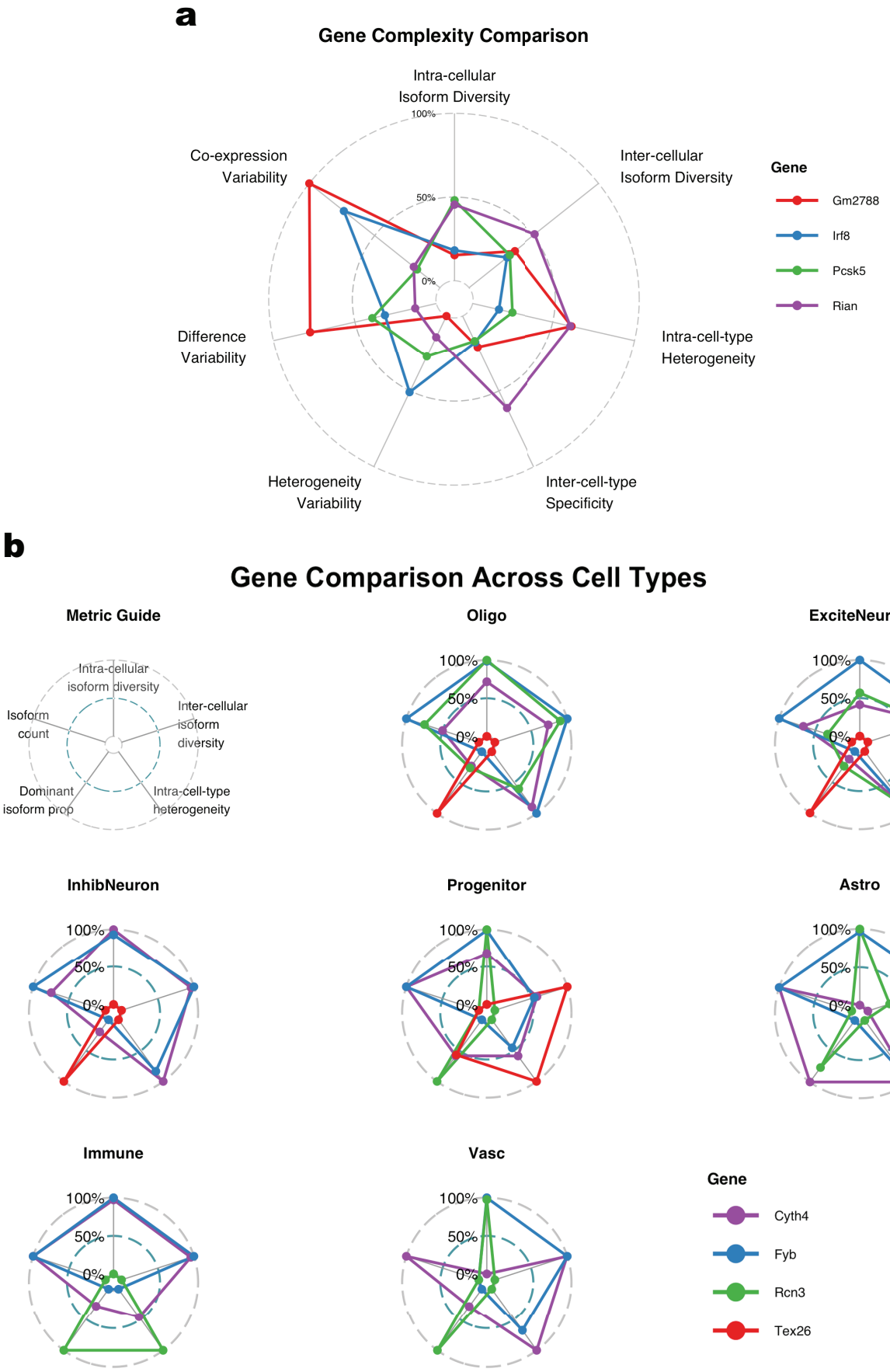
a
Gene Complexity Comparison
Intra-cellular Isoform Diversity
Inter-cellular Isoform Diversity
Intra-cell-type Heterogeneity
Inter-cell-type Specificity
Heterogeneity Variability
Difference Variability
Co-expression Variability
100%
50%
0%
Gene
Gm2788
Irf8
Pcsk5
Rian
b
Gene Comparison Across Cell Types
Metric Guide
Intra-cellular isoform diversity
Inter-cellular isoform diversity
Intra-cell-type heterogeneity
Dominant isoform prop
Isoform count
Oligo
ExciteNeuron
InhibNeuron
Progenitor
Astro
Immune
Vasc
Gene
Cyth4
Fyb
Rcn3
Tex26

Supplementary Figure 3: **Radar chart visualisations for multidimensional complexity comparisons.** (a) Seven-dimensional complexity metric comparison radar charts for four genes (*Gm2788*, *Irf8*, *Pcat5*, and *Ran*) in the mouse early blood development dataset, showcasing the unique complexity signatures of different genes. Each gene displays a distinctive complexity fingerprint, reflecting its specific isoform regulatory mechanisms. (b) Complexity profiles of individual genes (*Fyb*, *Mxra8*, *Rcn3*, and *Tex26*) across eight different brain cell types visualised with radar charts, demonstrating cell type specificity of isoform regulation. A metric guide in the top-left corner provides the meaning of the five axes in the radar charts. This visualisation method effectively captures and compares high-dimensional complexity data. Immune - immune cells; Astro - astrocytes; Oligo - oligodendrocytes; ExciteNeuron - excitatory neurons; InhibNeuron - inhibitory neurons; Progenitor - progenitor cells; Vasc - vascular cells.

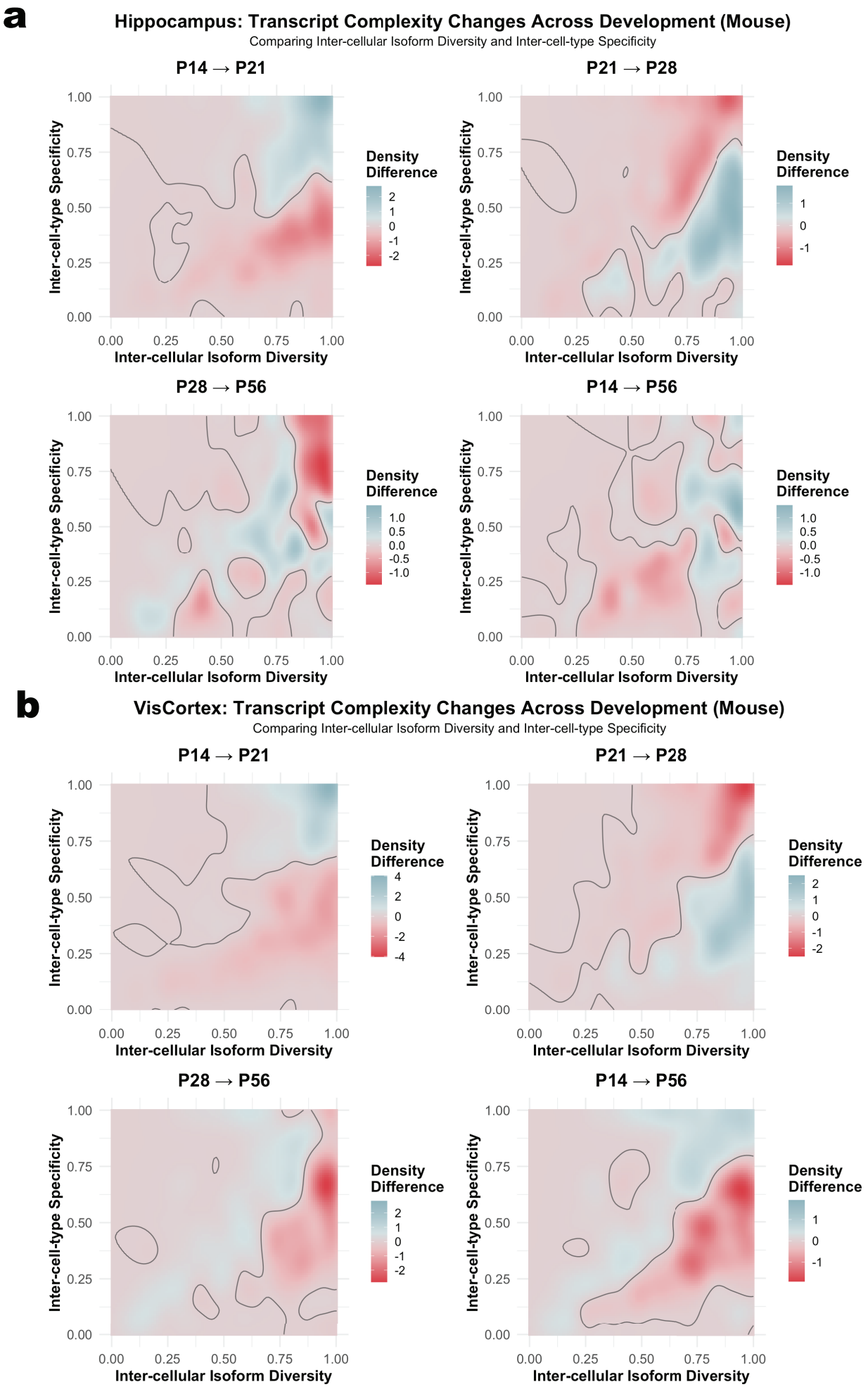
a
Hippocampus: Transcript Complexity Changes Across Development (Mouse)
Comparing Inter-cellular Isoform Diversity and Inter-cell-type Specificity
P14 → P21
P21 → P28
P28 → P56
P14 → P56
Inter-cell-type Specificity
Inter-cellular Isoform Diversity
Density Difference
b
VisCortex: Transcript Complexity Changes Across Development (Mouse)
Comparing Inter-cellular Isoform Diversity and Inter-cell-type Specificity
P14 → P21
P21 → P28
P28 → P56
P14 → P56
Inter-cell-type Specificity
Inter-cellular Isoform Diversity
Density Difference

Supplementary Figure 4: **Dynamic changes in transcriptomic complexity across postnatal developmental stages in mouse hippocampus and visual cortex regions.** (a) Density difference maps comparing inter-cellular isoform diversity and inter-cell-type specificity in mouse hippocampus across four developmental stages (Days 14, 21, 28 and 56). Red regions indicate gene decreasing density while blue regions indicate increasing density. Each transition period shows a unique pattern of changes. (b) Complexity change patterns in mouse visual cortex across four developmental stages, showing region-specific differences compared to hippocampus. Colour scales indicate the intensity of density differences. This analysis reveals spatiotemporal-specific changes in transcriptomic complexity during brain development.

a **Transcript Complexity Differences Between Mouse Brain Regions Across Different Time Points**

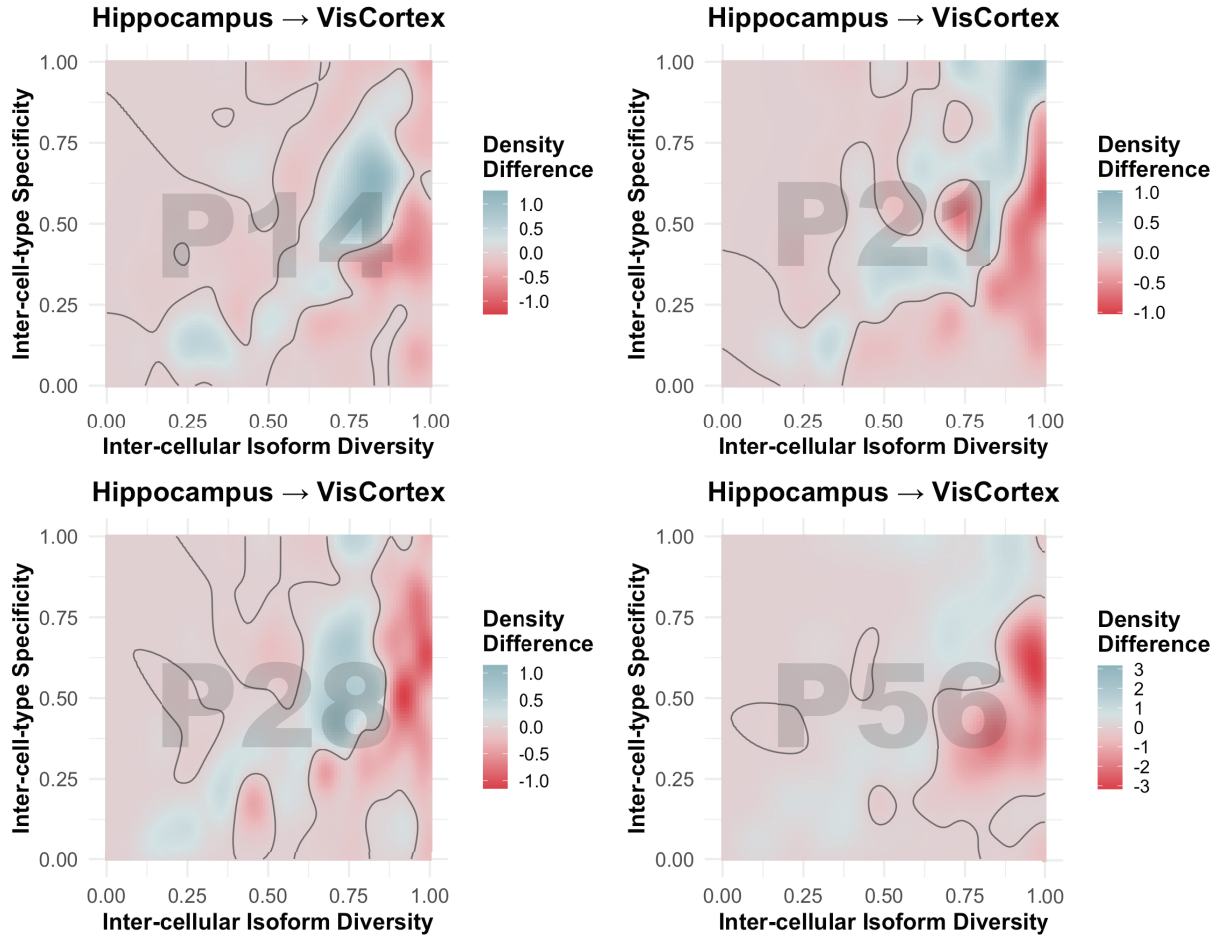

b **Transcript Complexity Differences Between Adult Human Brain Regions**

Comparing Inter-cellular Isoform Diversity and Inter-cell-type Specificity

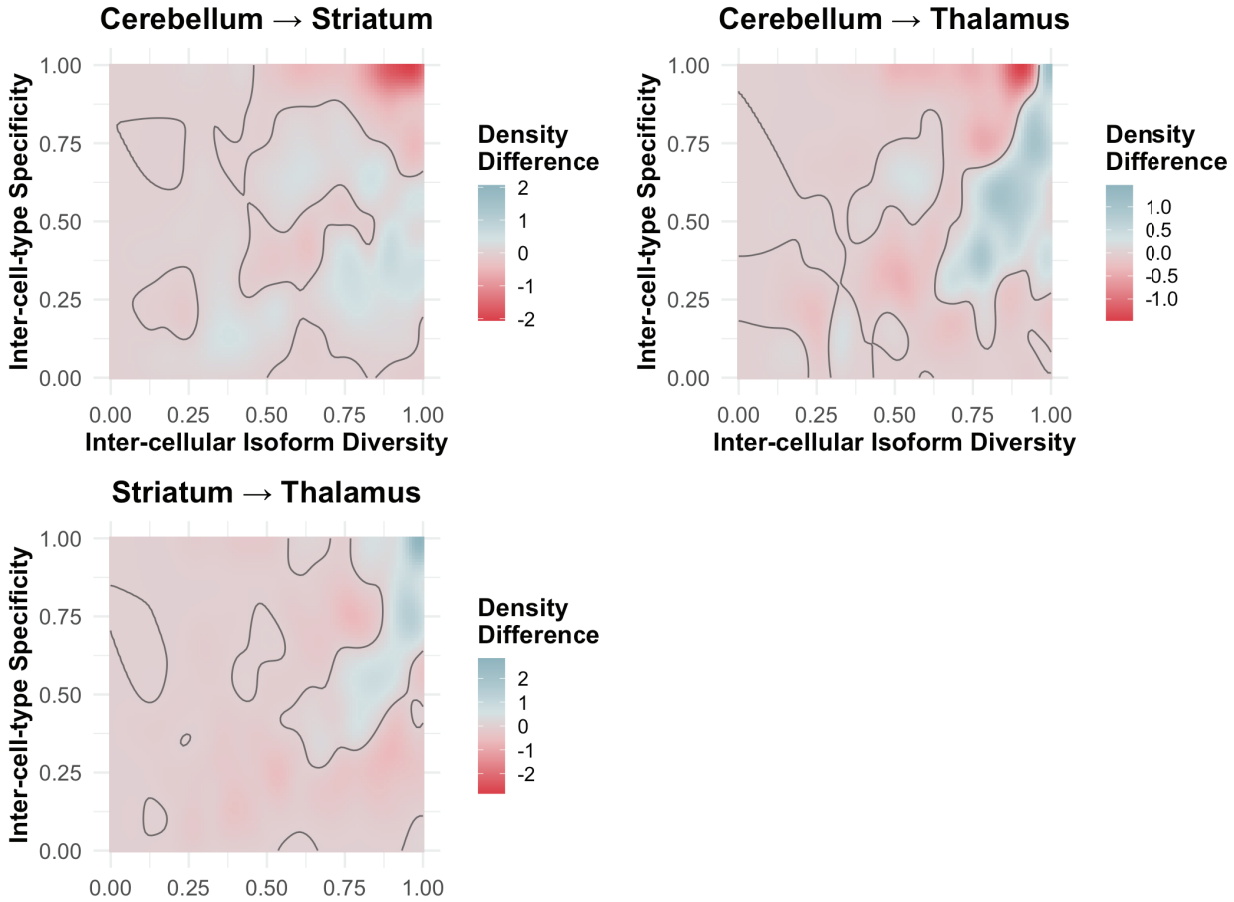

Supplementary Figure 5: **Transcript complexity differences between mouse brain regions across postnatal developmental stages and between adult human brain regions.** (a) Developmental changes in transcript complexity profiles comparing hippocampus and visual cortex regions across different time points in mouse brain (Days 14, 21, 28 and 56). Each density difference map displays changes in the relationship between inter-cellular isoform diversity and inter-cell-type specificity, with blue indicating regions of increased gene density and red indicating decreased density. These developmental comparisons reveal dynamic shifts in transcriptomic complexity patterns as brain circuits mature. (b) Transcript complexity differences between adult human brain regions. The figure presents density difference maps between three pairs of distinct brain regions (Cerebellum-Striatum, Cerebellum-Thalamus, and Striatum-Thalamus). Each comparison displays regional differences in inter-cellular isoform diversity and inter-cell-type specificity, with blue indicating greater gene density in the first region and red indicating greater density in the second region.

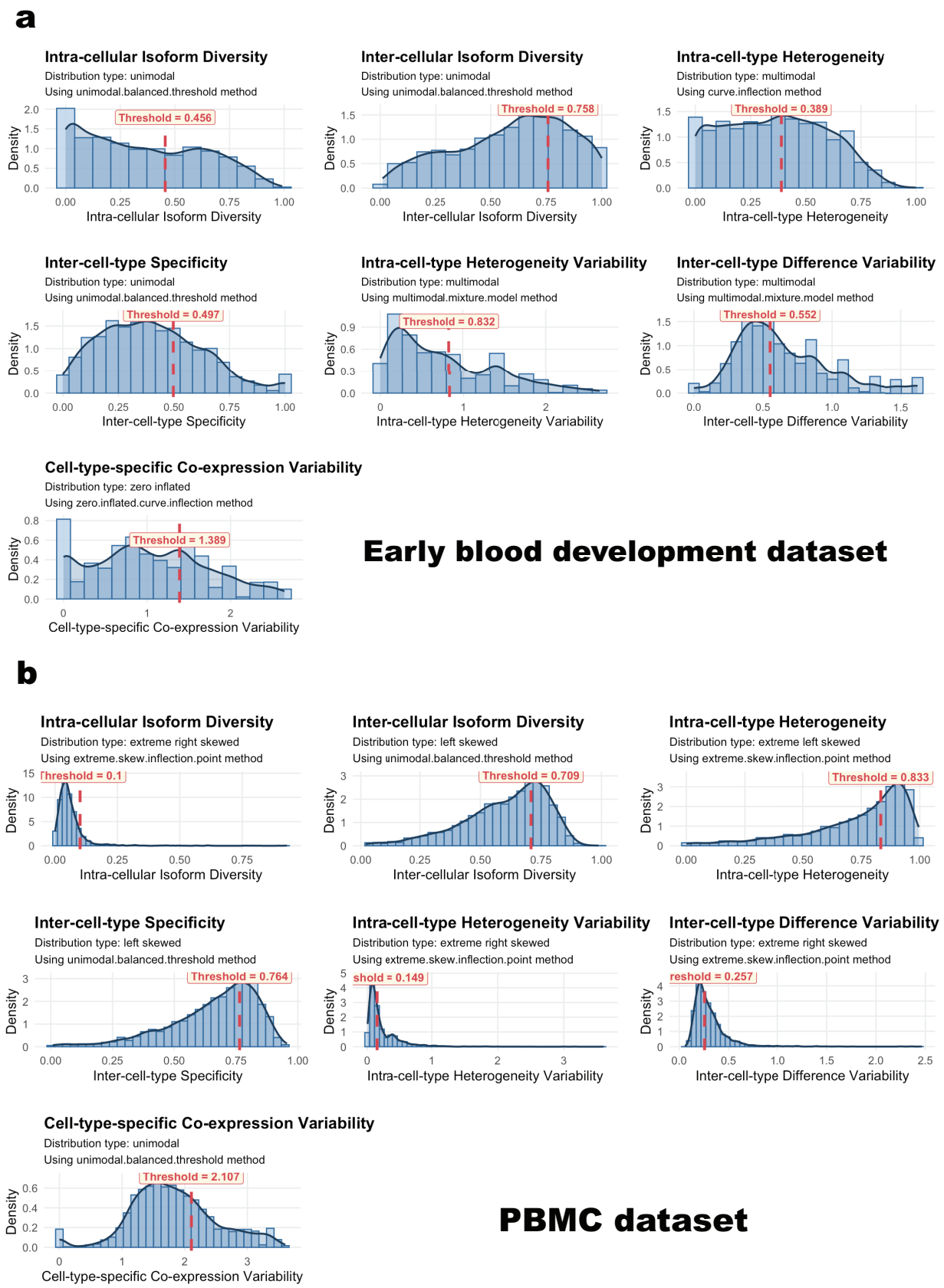

Supplementary Figure 6: **Visualisation of complexity metric threshold determination for early blood development and PBMC datasets.**

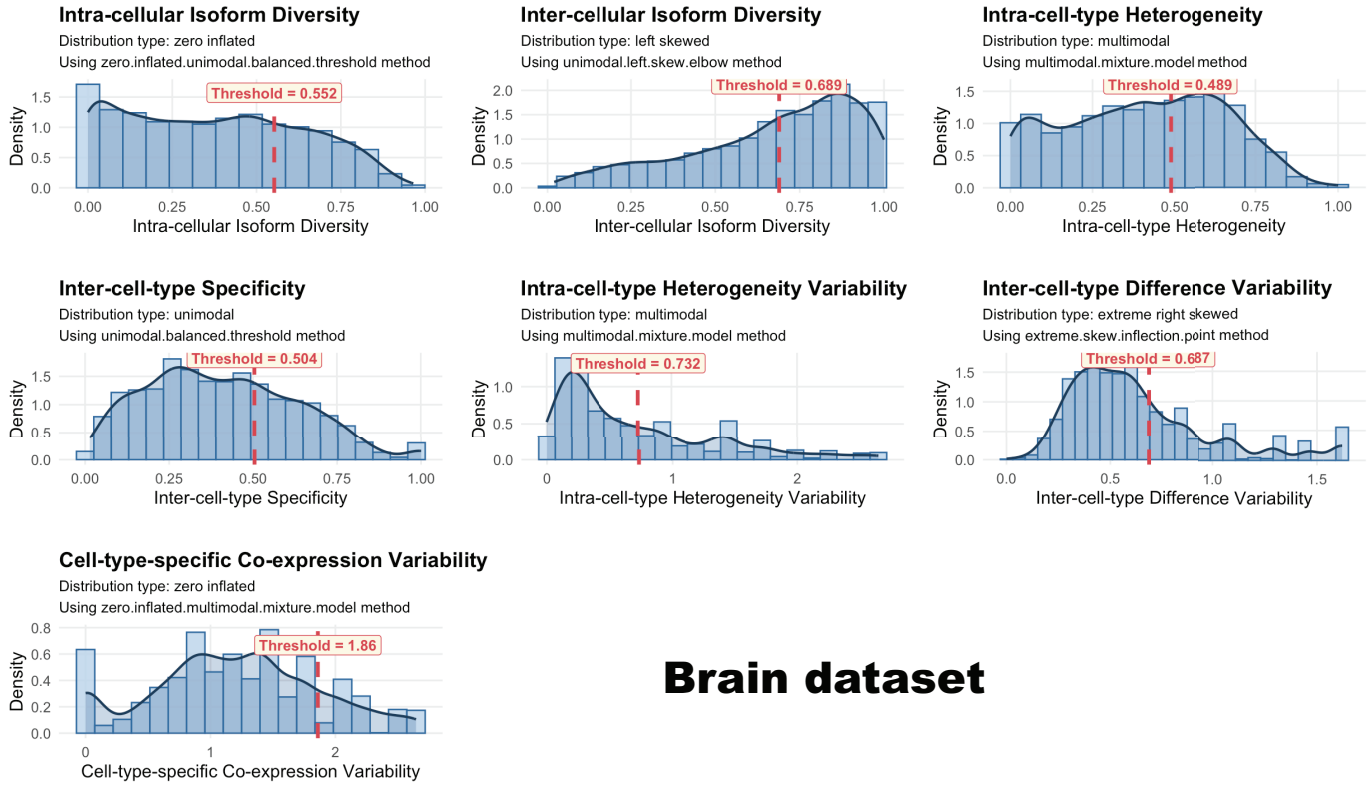

Supplementary Figure 7: **Visualisation of complexity metric threshold fitting for brain dataset.**